FOXC1 maintains the hair follicle stem cell niche and governs stem cell quiescence to preserve long-term tissue-regenerating potential

Kenneth Lay[a], Tsutomu Kume[b], and Elaine Fuchs[a,1]

[a]Howard Hughes Medical Institute, Laboratory of Mammalian Cell Biology and Development, The Rockefeller University, New York, NY 10065; and [b]Department of Medicine, Feinberg Cardiovascular Research Institute, Northwestern University School of Medicine, Chicago, IL 60611

Contributed by Elaine Fuchs, January 29, 2016 (sent for review January 11, 2016; reviewed by Angela Christiano, Pierre A. Coulombe, and Valerie Horsley)

Adult tissue stem cells (SCs) reside in niches, which orchestrate SC behavior. SCs are typically used sparingly and exist in quiescence unless activated for tissue growth. Whether parsimonious SC use is essential to conserve long-term tissue-regenerating potential during normal homeostasis remains poorly understood. Here, we examine this issue by conditionally ablating a key transcription factor Forkhead box C1 (FOXC1) expressed in hair follicle SCs (HFSCs). FOXC1-deficient HFSCs spend less time in quiescence, leading to markedly shortened resting periods between hair cycles. The enhanced hair cycling accelerates HFSC expenditure, and impacts hair regeneration in aging mice. Interestingly, although FOXC1-deficient HFs can still form a new bulge that houses HFSCs for the next hair cycle, the older bulge is left unanchored. As the new hair emerges, the entire old bulge, including its reserve HFSCs and SC-inhibitory inner cell layer, is lost. We trace this mechanism first, to a marked increase in cell cycle-associated transcripts upon *Foxc1* ablation, and second, to a downstream reduction in E-cadherin–mediated inter-SC adhesion. Finally, we show that when the old bulge is lost with each hair cycle, overall levels of SC-inhibitory factors are reduced, further lowering the threshold for HFSC activity. Taken together, our findings suggest that HFSCs have restricted potential in vivo, which they conserve by coupling quiescence to adhesion-mediated niche maintenance, thereby achieving long-term tissue homeostasis.

stem cells | hair follicle | FOXC1 | quiescence | aging

Adult stem cells (SCs) are endowed with the remarkable ability to make, maintain, and repair tissues. As such, they are tasked with maintaining tissue homeostasis throughout the lifetime of the organism. In order for them to fulfill this responsibility, SCs are kept in a quiescent state in between their utilization. This reduces their exposure to metabolic and replicative stress, thereby preserving their genomic integrity (1, 2).

A key provider of regulatory signals that balance SC quiescence and activity is the SC environment. Termed the "niche," it not only provides a residence for SCs, but also interacts with SCs to regulate their behavior and properties (3, 4). Niche signals can take the form of short-range cues from the immediate neighbors of the SCs, or longer-range signals from the macroenvironment of the organ (5–8). Together, these signals ensure that SCs are used efficiently to meet tissue-specific physiological needs. Whether this efficiency of SC use guarantees their potential to make tissues long term remains largely unexplored.

The mouse pelage hair follicle (HF) is an excellent model to investigate the importance of SC quiescence and the mechanisms that regulate it. These HFs undergo hair cycles, which are periodic bouts of regeneration (anagen), degeneration (catagen), and rest (telogen) (Fig. S1*A*). Long-term SCs of the HF (HFSCs) reside in an anatomically defined region of the HF termed the bulge (Bu). Bu-HFSCs are used infrequently, spending much of the hair cycle in quiescence. During early anagen, Bu-HFSCs enter a brief proliferative phase to self-renew and generate shorter-lived progeny, which then fuel the further maturation of the HF and production of new hair. Bu-HFSCs then return to quiescence by midanagen and remain in this state until the next hair cycle. Therefore, be it during the resting or regenerative phases of the hair cycle, Bu-HFSC activity is tightly controlled, making the HF an ideal system to investigate how SCs are kept in quiescence and activated only to the extent that is sufficient for successful tissue regeneration.

Like other adult SC niches, the bulge environment is rich in various inhibitory and activating signals that influence SC behavior. Multiple heterologous cell types contribute to HFSC quiescence, including the fibroblasts in the surrounding dermis, and underlying subcutaneous adipocytes, both of which secrete bone morphogenetic proteins (BMPs) that restrict HFSC activity (9, 10). Another potent source of inhibitory factors, in the form of BMP6 and FGF18, comes from the HFSC-derived keratin 6 (K6)-positive cell layer within the bulge (11). Together, these strong inhibitory signals keep HFSCs in quiescence. On the other hand, activating signals emanate mainly from the mesenchymal dermal papilla (DP) located at the base of each HF. During the resting phase, cross-talk between the DP and HFSCs leads to an accumulation of stimulatory factors. When these signals override the inhibitory ones, HFSCs at the bulge base (hair germ, HG) begin to proliferate, and hair regeneration is initiated. Soon thereafter, Bu-HFSCs self-renew and generate the outer root sheath (ORS), which distances the DP stimulus from the bulge as

Significance

Stem cells (SCs) of the hair follicle (HF) undergo cyclical bouts of activity during which hair regeneration occurs. They reside in a specialized niche, the bulge, which confers upon them extended periods of quiescence. Here, we identify Forkhead box C1 (FOXC1) as a key transcriptional regulator of HFSC activity and bulge maintenance. Loss of FOXC1 reduces the threshold for HFSC activation, causing excessive HFSC usage and dramatically shortening periods between hair growth cycles. Additionally, signs of weakened cellular junctions are seen within the niche, resulting in mechanically induced, premature loss of established hairs along with some SCs. The consequences of these defects are dire for aging animals, which display diminished HFSC niches and a sparse hair coat.

Author contributions: K.L. and E.F. designed research; K.L. performed research; T.K. contributed Foxc1-flox mice; K.L. and E.F. analyzed data; and K.L. and E.F. wrote the paper.

Reviewers: A.C., Columbia University; P.A.C., The Johns Hopkins University; and V.H., Yale University.

The authors declare no conflict of interest.

Freely available online through the PNAS open access option.

Data deposition: The data reported in this paper have been deposited in the Gene Expression Omnibus (GEO) database, www.ncbi.nlm.nih.gov/geo (accession no. GSE77256).

[1]To whom correspondence should be addressed. Email: fuchslb@rockefeller.edu.

This article contains supporting information online at www.pnas.org/lookup/suppl/doi:10.1073/pnas.1601569113/-/DCSupplemental.

www.pnas.org/cgi/doi/10.1073/pnas.1601569113

the HF grows downward (Fig. S1*A*). In this way, HFSCs in the bulge and along the upper ORS return to their quiescent state.

The first telogen (postnatal day ~P19) lasts only 2–3 d. Once the next regenerative phase is complete, most of the cells within the HF apoptose and regress, during which some Bu-HFSC progeny survive to construct a new bulge, again consisting of an outer layer of Bu-HFSCs and inner layer of $K6^+$ inhibitory cells (Fig. S1*A*).

A unique property of the murine pelage HF is its maintenance of the older bulge alongside the newly made one (Fig. S1*A*). The old bulge retains the club hair from the previous hair cycle, providing a means for the animal to build and maintain a thicker hair coat. HFSCs within the old bulge act as reserve SCs and are capable of repairing wounded epidermis (11). Because there is only one DP, only HFSCs of the new bulge participate in hair regeneration.

Although anagen and catagen are similar irrespective of the hair cycle, each telogen becomes significantly longer with age. Notably, in contrast to the initial 2- to 3-d quiescence period in one-bulge HFs, Bu-HFSCs residing in HFs with two or more bulges remain quiescent for weeks, even months, without launching a new hair cycle (Fig. S1*A*). A multitude of signals act to restrict HFSC activity, but whether maintaining older bulges contributes to prolonging the resting phases of later hair cycles remains unknown (11). Here, we address whether the old bulge influences stem cell use and activity, and we delineate the consequences that arise when HFSCs are triggered to regenerate tissues excessively.

We segued into these fascinating questions in the course of our characterizing transcription factors that govern HFSC characteristics and behavior. We identified *Foxc1*, a gene encoding the transcription factor Forkhead box C1 (FOXC1), as an early transcription factor expressed during developing HFs (12) and in adult Bu-HFSCs (13), and as a downstream target of BMP-pSMAD1 signaling (14). Upon conditionally ablating *Foxc1* from HFs, we discovered that HFs lose the ability to maintain their old bulge in part because of a reduction in E-cadherin at SC intercellular junctions. Therefore, although each *Foxc1*-mutant hair cycle generates a new functional bulge and club hair, the previous bulge—including its club hair, reserve SC pool, and SC-inhibitory $K6^+$ cells—is never retained. Probing the mechanism, we show that when WT HFs are imposed to have only a single bulge, they display a shortened resting phase and launch precocious hair cycling. In FOXC1-deficient HFs, the telogen phase is even shorter than WT HFs with only a single bulge. We trace this difference to transcriptional increases in cell cycle genes expressed by *Foxc1*-cKO Bu-HFSCs, which in turn account for their reduced E-cadherin levels and subsequent failure to maintain the bulge. Overall, the excessive rounds of hair regeneration seen in *Foxc1*-cKO mice have dire consequences. As the mice age, their Bu-HFSCs are unable to maintain their numbers, resulting in a thinning of the hair coat and a marked delay in regenerating new hairs.

Results

Depletion of FOXC1 Results in Faster Hair Cycling and Impacts Long-Term Hair Coat Maintenance. FOXC1 was expressed at all stages of the hair cycle in Bu-HFSCs, $K6^+$ inner bulge layer, isthmus, and sebaceous gland (Fig. 1*A*). In anagen, FOXC1 was also expressed in the differentiated inner root sheath that encases the new hair shaft, whereas in catagen, it was observed in the regressing portion of the HF (Fig. S1*B*). In $K14Cre^{Tg/WT} \times Foxc1^{fl/fl}$ mice, FOXC1 was absent throughout skin epithelia (hereafter referred to as WT vs. *Foxc1*-cKO), whereas expression of other key HFSC transcription factors and overall skin architecture were intact (Fig. S1*C*).

To observe hair cycle progression under native conditions, we shaved the dorsal back of mice after each round of hair cycling, starting from the first hair coat in first telogen at P19. This allowed us to pinpoint the hair cycle stage according to the transition of skin color from pink (telogen) to grey (anagen) (15). Generation of a second hair coat and entry into the second telogen occurred normally, suggesting that anagen and catagen were unperturbed by loss of FOXC1. However, *Foxc1*-cKO mice entered their next anagen and regenerated their third hair coat dramatically earlier than WT littermates (Fig. 1*B*). Indeed, incorporation of BrdU confirmed the precocious proliferation of *Foxc1*-cKO HFSCs, indicating a shortening of the typically extended second telogen (Fig. 1*C*).

In subsequent hair cycles, *Foxc1*-cKO mice continued to display significantly shortened telogens relative to their WT counterparts. By 9 mo of age, many *Foxc1*-cKO mice were in their seventh telogen, whereas WT mice were still in their fourth telogen (Fig. 1 *D* and *E*). By these criteria, the major defect arising from loss of FOXC1 appeared to be a failure to maintain extended telogens, resulting in a dramatic increase in the frequency of hair cycling through most of the lifetime of the animal.

Despite the overall markedly abridged telogens, *Foxc1*-cKO HFs still experienced a modest age-related extension in telogen length, a feature that is more conspicuous in WT HFs and that has been attributed to a rise in macro-BMP levels in aging skin (10) (Fig. 1*D*). However, in contrast to their WT counterparts, even though young *Foxc1*-cKO mice generated grossly normal hair coats, their hair coats became sparser and frequently greyed as they aged (Fig. 1*F*). This finding suggested that the bulge niche and its residents might be functionally impacted through excessive utilization during frequent hair cycling.

FOXC1 Is Necessary to Establish a Multiple-Bulge HF Architecture, and Maintain HFSC Numbers and Function with Age. To explore the consequences of FOXC1 loss further, we quantified Bu-HFSC numbers in young (P19, first telogen, and P42, second telogen) and aged (≥1.5 y) mice. In first telogen, both WT and *Foxc1*-cKO HFs had one bulge with no significant differences in Bu-HFSC numbers. However, in second telogen, although WT HFs had established a two-bulge architecture, *Foxc1*-cKO HFs still had only one bulge and failed to expand their Bu-HFSC numbers like WT HFs did (Fig. 2 *A*–*C*). This one-bulge phenotype persisted in subsequent hair cycles: whereas WT HFs had up to three and four bulges in third and fourth telogen, respectively, *Foxc1*-cKO HFs continued to maintain only one (Fig. 2*D*).

Once an old club hair is shed, the bulge structure disappears. Therefore, in aged mice, WT HFs continued to maintain a two-to-four bulge architecture, whereas *Foxc1*-cKO HFs still had only one bulge. Notably, their bulges were frequently smaller and contained dramatically fewer Bu-HFSCs compared with both aged WT HFs and young *Foxc1*-cKO HFs (Fig. 2 *C* and *E*). By these criteria, starting from the second telogen, *Foxc1*-cKO Bu-HFSC numbers appeared to wane with subsequent hair cycles.

To test the ability of aged *Foxc1*-cKO HFSCs to regenerate hairs, we depilated the hair coat, which removes the club hair and its associated $K6^+$ inner bulge layer, to stimulate HFSC proliferation and anagen entry (11). Interestingly, both young and aged *Foxc1*-cKO HFSCs proliferated 1 d earlier than their WT counterparts (Figs. 2 *F* and *G*). However, by ~5 d post-depilation, young and aged WT HFs and young *Foxc1*-cKO HFs had progressed to midanagen, but some aged *Foxc1*-cKO HFs were still in early anagen, even though their HFSCs in the bulge and upper ORS showed signs of proliferation (Fig. 2*H*). Consequently, despite an initial accelerated response, aged *Foxc1*-cKO HFSCs regenerated a hair coat more slowly than their aged WT and young mutant counterparts, suggesting a functional decline (Fig. 2*I*).

FOXC1-Deficient HFs Can Make a New Bulge but Fail to Maintain the Older One. Intrigued by the one-bulge phenotype, we wanted to know how it arises, and if it results in more than just thinning of the hair coat. We first determined whether FOXC1-deficient HFs failed to establish their new bulge or precociously lost their old one. To test the former, we labeled their lower ORS cells by

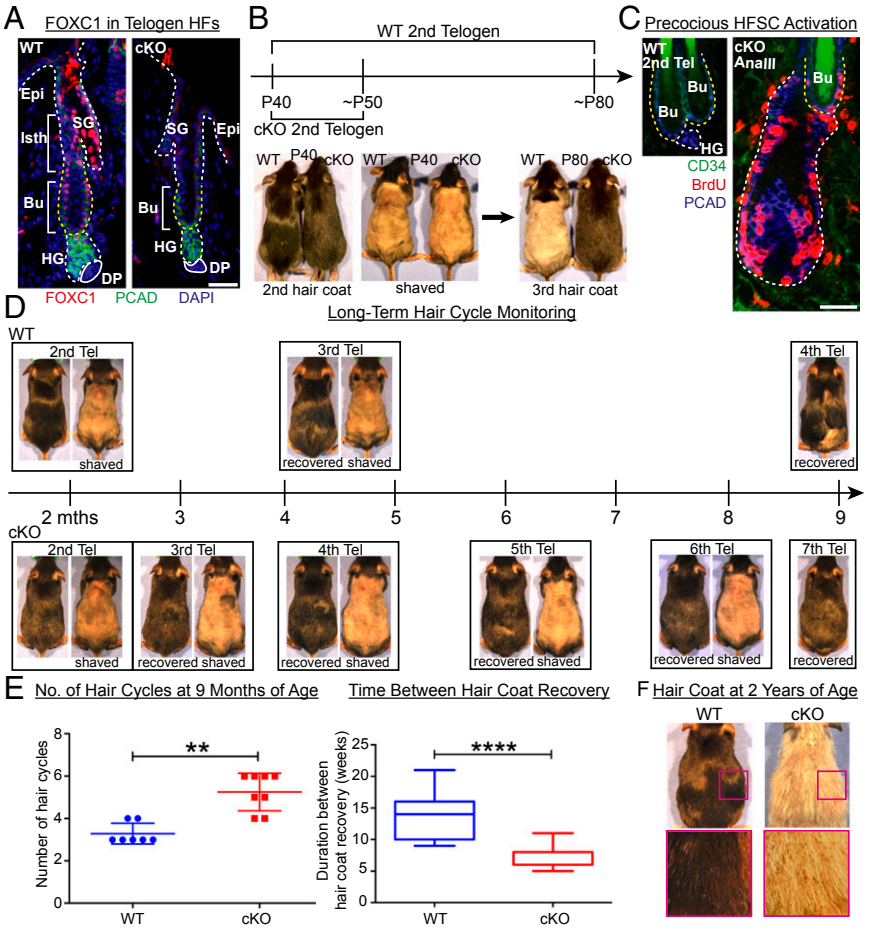

Fig. 1. Depletion of FOXC1 from HFs causes faster hair cycling, yielding a sparser hair coat with age. (*A*) Validation of *Foxc1*-cKO by immunofluorescence. Abs are color-coded according to the fluorescent secondary Abs used. Bu, bulge; DP, dermal papilla; Epi, epidermis; HG, hair germ; Isth, isthmus; SG, sebaceous gland. (Scale bar, 30 μm.) (*B*) *Foxc1*-cKO mice regenerated their third hair coat much earlier than WT mice. (*C*) Immunofluorescence of *Foxc1*-cKO HF sagittal section at P50, depicting precocious Bu-HFSC activation and earlier entry into anagen than WT. (Scale bar, 30 μm.) (*D*) Recovered hair coats of WT (*Top*) and *Foxc1*-cKO (*Bottom*) were shaved repeatedly to monitor hair cycles long-term. Tel, telogen. (*E*) *Foxc1*-cKO mice underwent more frequent hair cycling and exhibited significantly shorter intervals between hair cycles. (*Left*) Data are mean ± SD. $^{**}P < 0.01$. (*Right*) "Duration between hair coat recovery" refers to the time taken for > 80% of the hair coat to recover after shaving; box-and-whisker plot: midline, median; box, 25th and 75th percentiles; whiskers, minimum and maximum. $^{****}P < 0.0001$. (*F*) Representative example of hair coat of WT and *Foxc1*-cKO mice at 2 y of age. Pink box indicates zoomed-in view of lateral side of hair coat. Note visibility of skin (with some pigmented spots) underneath a sparse hair coat in *Foxc1*-cKO.

administering BrdU in late anagen, long after the bulge had ceased proliferation. In WT HFs, some of these BrdU-labeled ORS cells survived the ensuing catagen and made the $K6^+$ inner layer of the new bulge, whereas the old bulge remained unlabeled (11). In *Foxc1*-cKO HFs, the single bulge displayed BrdU-retaining $K6^+$ cells, indicating that it was newly formed (Fig. S2*A*).

To confirm that the old bulge was lost, we traced the old club hair by dyeing it in first telogen and tracking it through first anagen (Fig. S2*B*). In late anagen, the dyed hairs of WT HFs persisted, but many of the hairs in *Foxc1*-cKO HFs were gradually lost (Fig. S2*C*). Immunofluorescence confirmed that in second telogen, WT HFs consisted of an old bulge that anchored a dyed hair and a new bulge that anchored a nondyed hair; in contrast, *Foxc1*-cKO HFs consisted of a single new bulge anchoring a nondyed hair (Fig. S2*B*). These data indicated that with every hair cycle, *Foxc1*-cKO HFs were able to generate a new bulge but failed to maintain the old one.

Preservation of the Old Bulge Contributes to SC Quiescence. To investigate whether the old bulge plays a functional role in regulating hair cycling, we forced WT HFs to lose their old bulge precociously, thereby phenocopying *Foxc1*-cKO HFs. To do so, we depilated them in first telogen to remove the club hair and inner $K6^+$ bulge layer, and then allowed them to generate a new bulge and club hair. We also shaved the undepilated posterior region to monitor natural hair cycle progression (Fig. 3 *A* and *B*). Both depilated and undepilated halves generated new hairs and entered second telogen by ~P40 (Fig. 3*B*). However, although the posterior HFs now had two bulges, the anterior HFs had only one (Fig. 3*C*).

We then shaved the new hairs to continue monitoring the hair cycle. Whereas the posterior two-bulge HFs stayed in second telogen for ~6.5 wk, the anterior one-bulge HFs remained in second telogen for only ~2.5 wk before regenerating a full hair coat precociously (Fig. 3 *B* and *F*) (WT 2-Bu vs. WT 1-Bu). The anterior–posterior boundary was maintained throughout both hair cycles, indicating that precocious anagen occurred specifically in one-bulge HFs only. The converse experiment was repeated (posterior half, depilated; anterior half, shaved) with analogous results (Fig. S3*A*). Under the conditions used, HFs were age-, sex-, and strain-matched, thereby providing compelling evidence that the presence of the old bulge contributed to HFSC quiescence. Based upon the existing literature, we attribute this to the contribution of inhibitory signals, particularly FGF18 and BMP6,

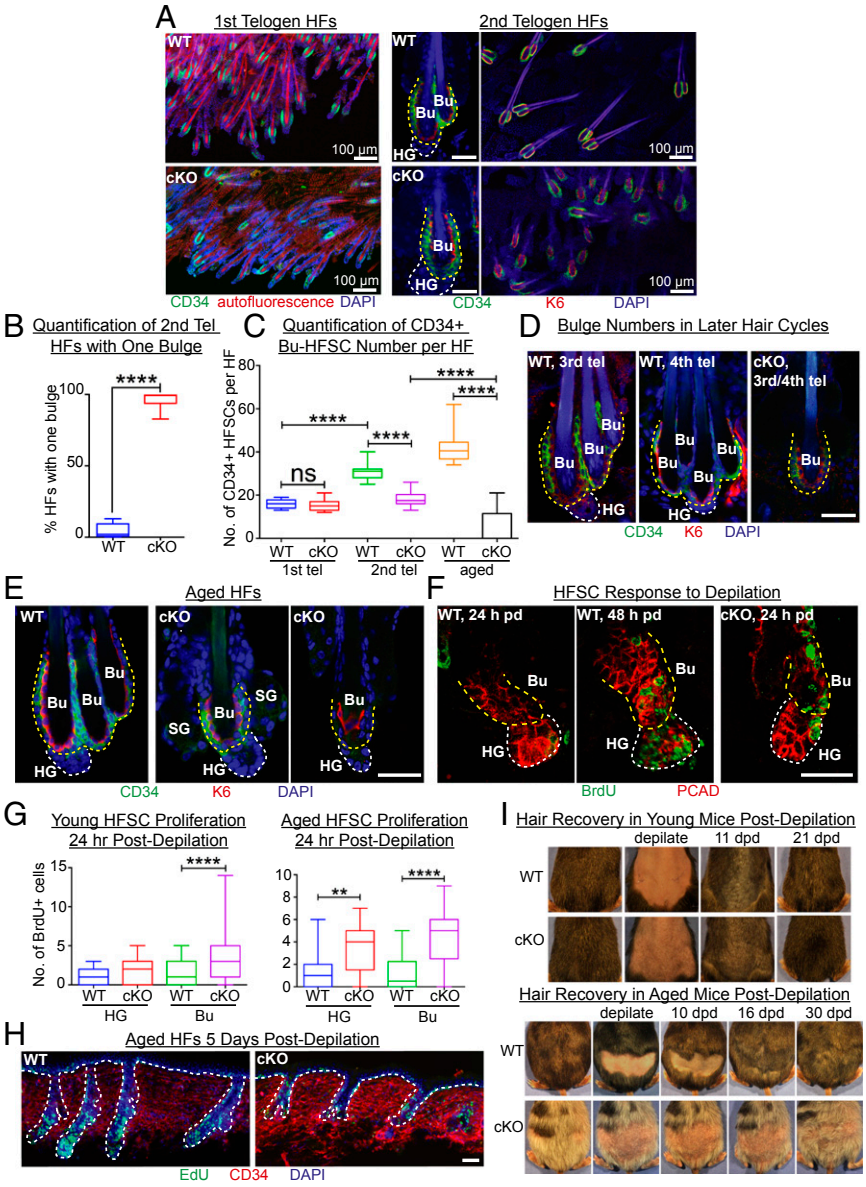

Fig. 2. Without FOXC1, HFs fail to maintain multiple bulges and club hairs and display reduced HFSCs. (*A*) Whole-mount immunofluorescence of WT and *Foxc1*-cKO first telogen (*Left*) and second telogen (*Right*) HFs. CD34 (green) marks outer bulge layer (HFSCs); K6 (red) marks inner bulge layer; red autofluorescence marks club hair. Bu, bulge; HG, hair germ. [Scale bars of magnified images (*Center*), 30 μm.] (*B*) Quantification of second telogen HFs with one bulge in dorsal skin ($n \geq 4$ mice, ≥80 HFs from each mouse). Box-and-whisker plot: midline, median; box, 25th and 75th percentiles; whiskers, minimum and maximum. ****$P < 0.0001$. (*C*) Quantification of total number of CD34$^+$ HFSCs (both basal-Bu and suprabasal-Bu) per whole-mount HF ($n \geq 2$ mice, ≥10 HFs per mouse). ****$P < 0.0001$; ns, nonsignificant. (*D*) Whole-mount immunofluorescence of WT and *Foxc1*-cKO HFs in third and fourth telogen. Note the increase in bulge numbers in WT but persistent one-bulge phenotype in *Foxc1*-cKO. CD34 expression is frequently weaker in *Foxc1*-cKO. (Scale bar, 30 μm.) (*E*) Whole-mount immunofluorescence of HFs in aged (≥1.5 y) WT and *Foxc1*-cKO animals. SG, sebaceous gland. (Scale bar, 30 μm.) (*F*) Sagittal section immunofluorescence of HFs which were depilated and then pulsed with BrdU for 24 h. Skin biopsies were retrieved at $t = 24$ and 48 h postdepilation. PCAD (P-cadherin) stains HG and outlines Bu. Note that both aged and young *Foxc1*-cKO HFs respond faster than WT. (Scale bar, 30 μm.) (*G*) Quantification of BrdU$^+$ cells in Bu and HG 24 h postdepilation ($n = 2$ mice, ≥10 HFs per mouse). **$P < 0.01$; ****$P < 0.0001$. (*H*) Sagittal sections from day 5 postdepilated mice indicated that aged *Foxc1*-cKO HFs progressed to regenerate new hairs more slowly than WT. (Scale bar, 30 μm.) (*I*) Tracking of hair coat recovery postdepilation. Note that despite the faster response to depilation, hair coat recovery, determined by darkening of skin and appearance of new hair, was delayed in aged *Foxc1*-cKO mice.

emanating from first, the suprabasal Bu-HFSCs, which arise from the interface between two adjacent bulges (13), and second, the K6$^+$ inner layer of the old bulge (11).

Consistent with this notion and with a prior report that *Foxc1* is a downstream target of BMP signaling in proliferative hair progenitors (14), we did not see significant changes in *Fgf18* and *Bmp6* transcripts on a per K6$^+$ inner bulge cell basis in *Foxc1*-cKO one-bulge HFs, but we confirmed a reduction of inner bulge cell numbers, in addition to the complete absence of suprabasal Bu-HFSCs (Fig. 3*D*). In this regard, the microenvironment of the FOXC1-deficient bulge was likely to be reduced over WT for these inhibitory factors, a feature that would allow stimulatory signals to overcome the threshold for HFSC activation more easily.

Despite the impact of the old bulge, its loss was not sufficient to fully account for the acutely constrained telogen observed in *Foxc1*-cKO HFs (Fig. 3*F*) (WT 1-Bu vs. cKO 1-Bu). Thus, it was important to determine whether FOXC1 loss alone was sufficient to elicit telogen shortening under conditions where two bulges existed. To accomplish this, we used *Sox9CreER* to induce *Foxc1* ablation in two-bulge HFs during second telogen and quantified telogen duration as time taken for at least 50% of dorsal skin to enter anagen (Fig. 3*E* and Fig. S3*B*). We found that loss of FOXC1 alone shortened the second telogen of these two-bulge HFs, but to a lesser extent than when coupled with loss of the bulge (Fig. 3*F*). It was important to note that these two-bulge *Foxc1*-mutant HFs maintained their old bulges when they precociously entered anagen, but would lose them later and display a one-bulge phenotype in their next telogen (Fig. S3 *C* and *D*). Taken together, these data suggest that loss of FOXC1 influenced HFSC activity in at least two different ways.

FOXC1 Re-Establishes and Maintains Quiescence of HFSCs After Their Activation. To explore HFSC-intrinsic effects resulting from the loss of FOXC1, we performed RNA sequencing (RNA-seq) on late anagen and second telogen Bu-HFSC populations purified by FACS. Transcripts [with fragments per kilobase per million mapped reads (FPKM) > 1] that were significantly up-regulated [$P < 0.05$, false-discovery rate (q-value) < 0.05] upon FOXC1 loss were enriched for those encoding cell cycle-associated proteins, be it in anagen or second telogen (Fig. 4*A*, Fig. S4, and Datasets S1 and S2).

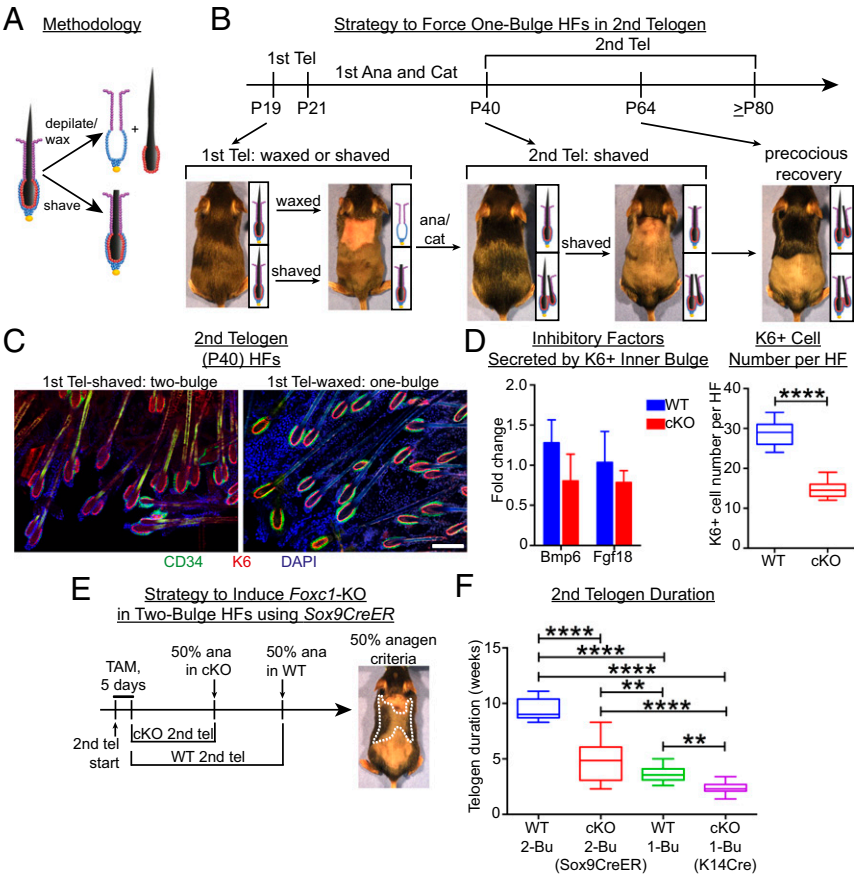

Fig. 3. The old bulge contributes to HFSC quiescence. (*A*) Methodology of hair-shaving and hair-depilation/waxing. Note that depilation of HF removes the club hair and associated $K6^+$ inner layer from the bulge, whereas shaving only clips away hairs at the skin surface. (*B*) Strategy to force WT second telogen HFs to have only one bulge. HF schematics next to mouse photos depict HF state after waxing/shaving and completion of anagen/catagen. First telogen (P19) HFs were depilated by waxing, and entered first anagen at the same time as their shaved counterparts. By second telogen (P40), shaved-HFs had two bulges/club hairs, but waxed-HFs had only one bulge/club hair. All HFs were then shaved to observe entry into second anagen. Ana, anagen; Cat, catagen; Tel, telogen. (*C*) Whole-mount immunofluorescence to validate strategy. Most first telogen-shaved-HFs had two bulges/club hairs, whereas first telogen-waxed HFs largely had one bulge/club hair only. (Scale bar, 100 μm.) (*D*, *Left*) qRT-PCR of SC-inhibitory factors from FACS-purified $K6^+$ inner bulge cells. Data are mean ± SEM. (*Right*) Quantification of $K6^+$ cell number per HF. Box-and-whisker plot: midline, median; box, 25th and 75th percentiles; whiskers, minimum and maximum ($n \geq 2$ mice, ≥10 HFs per mouse). Note that although *Bmp6* and *Fgf18* were only slightly reduced on a per cell level, there were fewer $K6^+$ inner bulge cells in FOXC1-deficient HFs, resulting in an overall reduced density of cells expressing these inhibitory factors. $^{****}P < 0.0001$. (*E*) Strategy to induce *Foxc1*-KO in second telogen two-bulge HFs using *Sox9CreER*. Mice were treated with tamoxifen for 5 d and observed for progression into anagen. Inset of mouse image depicts criteria to determine telogen duration, which was time taken for at least 50% of dorsal skin to enter anagen (as judged by greying, blackening or appearance of hair). (*F*) Second telogen duration determined by criteria described in *E*. WT two-bulge HFs, WT one-bulge HFs (postdepilation-recovery), *Foxc1-Sox9CreER*-cKO two-bulge HFs, and *Foxc1-K14Cre*-cKO one-bulge HFs were compared. Box-and-whisker plot: midline, median; box, 25th and 75th percentiles; whiskers, minimum and maximum ($n \geq 10$ mice). $^{**}P < 0.01$; $^{****}P < 0.0001$.

Cell cycle profiling performed on late anagen Bu-HFSCs confirmed that although WT Bu-HFSCs had largely returned to quiescence (G_0, as judged by DNA content and absence of Ki67) following their proliferative activity in early anagen, an appreciable fraction of FOXC1-deficient Bu-HFSCs remained in the cell cycle (non-G_0) (Fig. 4*B*). We observed a similar trend in second telogen, at a time when almost all WT Bu-HFSCs were in quiescence (Fig. 4*C*). Moreover, FACS-purified FOXC1-deficient Bu-HFSCs exhibited greater colony formation efficiency in vitro, analogous to that displayed by the more primed HG-HFSCs (16) (Fig. 4*D*). Given that loss of FOXC1 delayed the return of anagen Bu-HFSCs to quiescence, and also primed telogen Bu-HFSCs to proliferate precociously, our findings pointed to the view that FOXC1 acted to re-establish Bu-HFSC quiescence during anagen and maintain it during telogen.

Previously, it was shown that absence of the transcription factor NFATc1 causes de-repression of the cell cycle gene *Cdk4*, precocious HFSC activation, and hair cycling (17). Interestingly, when we conditionally ablated *Nfatc1* in HFs, we discovered that in addition to their precocious hair cycle entry, HFs also displayed a one-bulge phenotype (Fig. 4*E*). These data led us to hypothesize that upon loss of either FOXC1 or NFATc1, the SC-intrinsic proliferative activity itself may contribute to both faster hair cycling and loss of the bulge; the bulge loss in turn couples with this SC-intrinsic proliferative nature to further accelerate future hair cycles. We revisit this fascinating possibility again later.

FOXC1 Ensures Anchorage of Old Bulge to Prevent Its Loss During Anagen. Before exploring the possible relation between SC quiescence and bulge maintenance, we sought to understand how FOXC1 acts to preserve the old bulge. Because the old hairs were lost in anagen (Fig. S2*C*), we examined the genes that were significantly down-regulated in *Foxc1*-cKO anagen Bu-HFSCs before their loss, and found an enrichment of cell–cell and cell–extracellular matrix (ECM) adhesion transcripts, along with those encoding various intermediate filament components (Fig. S5 *A* and *B* and Dataset S1).

Hypothesizing adhesion to be the underlying defect causing the bulge loss, we tracked the fate of the old bulge and club hair using keratin 24 (K24). In first telogen, K24 was expressed specifically by Bu-HFSCs (Fig. S5*C*). In anagen, besides labeling the old Bu-HFSCs, K24 also labeled a region of the newly growing HF that was adjacent to the old bulge, hence marking the site of the future new bulge. Throughout WT anagen, the old bulge resided next to this new bulge site and below the sebaceous gland (Fig. 5*A*, *Upper*, and Fig. S5*D*).

In striking contrast, the *Foxc1*-cKO old bulge became separated from the new bulge site as the emerging new hair moved past it. As anagen progressed, the old bulge was seen above the sebaceous gland and sometimes even near the skin surface, being completely excluded from the new bulge region (Fig. 5*A*, *Lower*, and Fig. S5*D*). This process eventually resulted in the one-bulge HF observed in second telogen (Fig. S5*E*).

We further observed that this process sometimes left a trail of $K24^+$ cells behind the old bulge, suggesting that HFSCs were being lost along with it (Fig. 5*A*). Indeed, by flow cytometry, *Foxc1*-cKO HFs displayed few if any suprabasal Bu-HFSCs ($CD34^{Hi}\alpha6^{Lo}$) and a reduction in the proportion of basal Bu-HFSCs ($CD34^{Hi}\alpha6^{Hi}$) (Fig. 5*B*). Additionally, as quantified earlier, *Foxc1*-cKO Bu-HFSC numbers were lower than WT beginning in their second telogen (Fig. 2*C*).

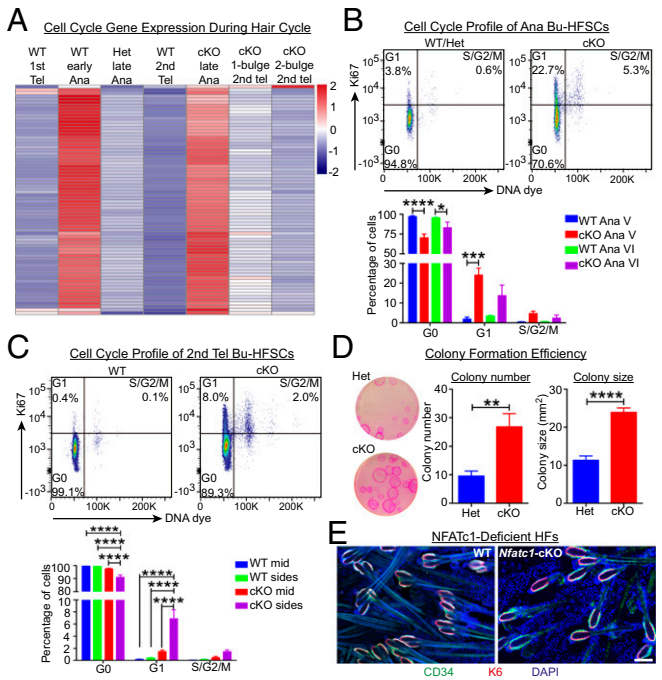

Fig. 4. FOXC1-mediated HFSC quiescence contributes to maintaining the old bulge. (*A*) Heat map to illustrate changes in expression of cell cycle genes (listed in Fig. S4*F*) through the first hair cycle. Ana, anagen; Tel, telogen. (*B*) Cell cycle analysis of late anagen (substages Ana V and Ana VI) Bu-HFSCs by flow cytometry and quantification of percentages of cells in various phases of the cell cycle. Ki67 marks cycling cells; DNA content distinguishes cells in $S/G_2/M$ from G_1/G_0). Data are mean ± SEM ($n \geq 3$ mice). $^*P < 0.05$; $^{***}P < 0.001$; $^{****}P < 0.0001$. (*C*) Cell cycle analysis of second telogen Bu-HFSCs by flow cytometry and quantification of percentages of cells in various phases of the cell cycle. "Mid" and "sides" refer to midline and lateral regions of dorsal skin from which cells were analyzed. Data are mean ± SEM ($n \geq 3$ mice). (*D*) Colony formation efficiency of *Foxc1*-cKO compared with $Foxc1^{+/-}$ Het Bu-HFSCs. (*Left*) Second telogen FACS-purified Bu-HFSCs were cultured in vitro for 2 wk and allowed to form colonies, which were then fixed and stained with Rhodamine B. (*Center*) Number of colonies formed per 33,000 cells plated. (*Right*) Area of each colony. Data are mean ± SEM ($n \geq 3$ mice, triplicates per mouse). $^{**}P < 0.01$; $^{****}P < 0.0001$. (*E*) Whole-mount immunofluorescence of *Nfatc1*-cKO HFs, showing a one-bulge phenotype. Because NFATC1 loss enhances Bu-HFSC proliferative activity, the one-bulge phenotype suggests that deregulation of quiescence may contribute to premature loss of the old bulge. (Scale bar, 100 μm.)

Finally, we performed a "hair-pull test" by applying an adhesive surgical tape and then peeling it off from the hair coat. Indeed, many more hairs came out from *Foxc1*-cKO than WT skin, indicating that *Foxc1*-cKO hairs were plucked out more easily than WT hairs (Fig. 5*C*). Taken together, these data suggest that FOXC1 functions in part to ensure adequate adhesion of the old bulge to prevent its loss during anagen.

Proliferative Bu-HFSCs Display Reduced E-Cadherin. Because loss of FOXC1 perturbed the transcription of genes encoding cell–ECM adhesion molecules, we FACS-purified Bu-HFSCs and tested their ability to adhere to different ECM components in vitro. Although cell–ECM adhesion defects could still be rooted in matrix production and organization, we did not observe significant differences in the ability of FOXC1-deficient and WT HFSCs to adhere to these various substrata (Fig. S6*A*).

On the other hand, our data presented in Fig. 4, along with the bulge-loss phenotype, raised the intriguing possibility of a possible link between SC-intrinsic proliferative behavior and a reduction in intercellular adhesion. These two cellular events often occur concomitantly in different biological contexts, prompting us to address whether the propensity of FOXC1-deficient Bu-HFSCs to proliferate might impact their intercellular adhesion.

We focused on E-cadherin, the central core of adherens junctions that are known to feature prominently in epithelial skin progenitors. In WT telogen HFs (Fig. 6*A*, *Left*), both basal (Fig. 6*A*, Inset a) and suprabasal (Fig. 6*A*, Inset b) $CD34^+$ Bu-HFSCs showed intense junctional E-cadherin immunolabeling, irrespective of whether they were in contact with themselves or with the inner $K6^+$ layer. However, in *Foxc1*-cKO HFs, junctional E-cadherin immunolabeling was reduced, especially at sites where Bu-HFSCs contacted each other (Fig. 6*A*, *Right*). This was intriguing given that E-cadherin's gene, *Cdh1*, was not affected transcriptionally by loss of FOXC1 (Fig. S6*B*). Additionally, the *Foxc1*-cKO bulge often consisted of three layers of disorganized and elongated cells, as opposed to the well-organized bilayer of compacted cells in WT bulge (Fig. 6*A*, *Right*).

We pursued these tantalizing hints at a relation between cell proliferation and intercellular adhesion by monitoring E-cadherin protein levels in WT Bu-HFSCs as they underwent the hair cycle (Fig. 6*B*). Interestingly, Bu-HFSCs displayed their highest levels of E-cadherin during telogen, while they were quiescent. In striking contrast, E-cadherin protein levels plummeted during early anagen as HFSCs became proliferative. Levels were up-regulated again as HFSCs returned back to quiescence in late anagen (Fig. 6*B*). In this way, E-cadherin protein (but not mRNA) (Fig. S6*B*) expression inversely correlated with cell-cycle gene expression, which was high in early anagen, down-regulated in late anagen, and further reduced in telogen (Fig. 4*A*).

Although *Foxc1*-cKO Bu-HFSCs exhibited similar E-cadherin expression dynamics, they exhibited lower levels than WT Bu-HFSCs at each stage throughout the hair cycle. This was especially evident in late anagen and telogen (Fig. 6*B*), a feature that corresponded to their atypical persistence in the cell cycle as revealed by RNA-seq and cell cycle profiling (Fig. 4). Taking these data together, we find that the failure of *Foxc1*-cKO Bu-HFSCs to return to quiescence and up-regulate E-cadherin promptly in late anagen could generate a mechanically weakened cell–cell adhesion state, which could account for the loss of the old bulge as the newly growing hair pushed passed it.

Direct Perturbation to Cell–Cell Adhesion Is Sufficient for Bulge Loss. Finally, to functionally test if reduction in E-cadherin was sufficient to cause the bulge loss in *Foxc1*-cKO HFs, we conditionally ablated *Cdh1*. Because $Cdh1^{fl/fl}$ × *K14Cre* mice exhibit early aberrations in HFs (18), we used *Sox9CreER* to efficiently induce *Cdh1* ablation in second telogen HFs. At this time, some HFs had begun to display a disorganized bulge with three cell layers, similar to that seen in *Foxc1*-cKO HFs (Fig. 6*A* and *C*). We then allowed HFs to progress from second telogen → second anagen → third telogen.

We checked for timing of second anagen entry. Unlike FOXC1 loss mediated by the same *Sox9CreER* (Fig. 3 *E* and *F*), E-cadherin loss did not result in precocious anagen, consistent with its putative role downstream of Bu-HFSC proliferation. However, like *Foxc1*-cKO HFs, as *Cdh1*-cKO HFs were undergoing their second anagen, their bulge was mis-localized relative to the newly specified bulge region (Fig. 6*D*). Moreover, as the old bulge moved upward, some $K24^+$ cells moved with it and were excluded from the new bulge region, whereas others were left behind ectopically (Fig. 6*D*, arrow).

Subsequently, by third telogen, like *Foxc1*-cKO HFs (Fig. S3 *C* and *D*), most *Cdh1*-cKO HFs displayed single bulges (Fig. 6*E*). Overall, with the exception of the precocious entry into the hair cycle, the bulge-loss phenotype seen with depletion of E-cadherin bore resemblance to that of *Foxc1*-cKO HFs.

Consistent with the fact that FOXC1-deficient Bu-HFSCs displayed only reduced and not silenced E-cadherin, the full *Cdh1* ablation in HFs resulted in a more severe phenotype, evident in

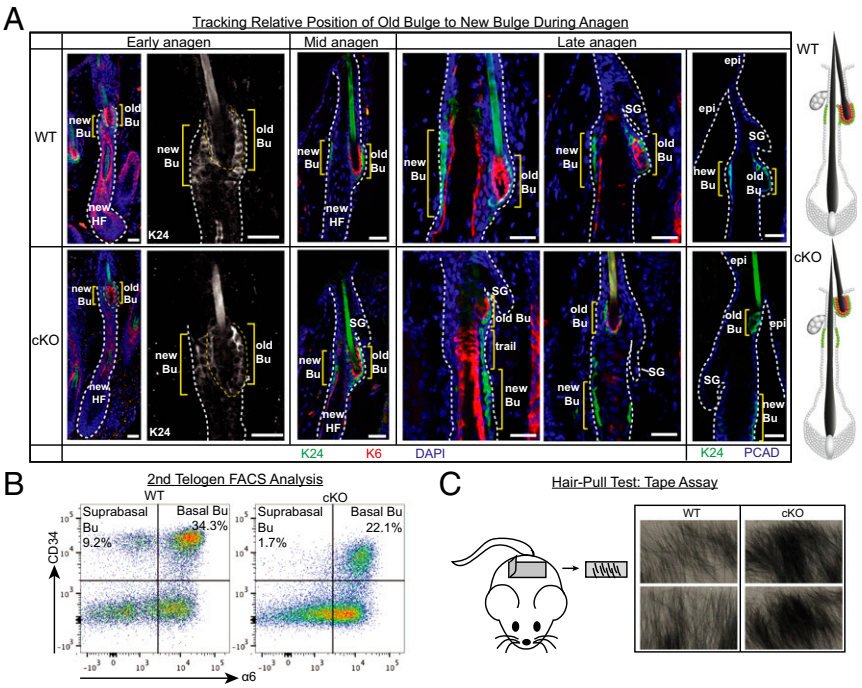

Fig. 5. FOXC1 functions to anchor the old bulge during hair growth. (*A*) Immunofluorescence of sagittal sections of anagen HFs. K24 marks the old-Bu-HFSCs and the new Bu region in newly growing HFs. K6 marks the inner layer of the old Bu and the companion layer of the new HF. PCAD (P-cadherin) marks the relatively undifferentiated progenitors of the HF, including those of the bulge, outer root sheath and sebaceous gland (SG). (Scale bars, 30 μm.) (*B*) Flow cytometry analysis of dorsal skin epithelial cells in second telogen. Depicted are singly dissociated HF cells that were negative for SCA1 (marker of basal epidermis) and positive for CD34 (surface marker of Bu-HFSCs) and α6 integrin (surface marker of all basal epithelial cells). Note that *Foxc1*-cKO HFs had only $CD34^{Hi}$ basal Bu-HFSCs, but lacked the suprabasal-Bu-HFSC population characteristic of the interface between two bulges. (*C*) Tape assay. A surgical tape was affixed to the hair coat, then peeled off to assess amount of hairs that came off with the tape (n = 3 mice).

their single bulge displaying an aberrant structure (Fig. 6*E*). Based upon these collective data, we conclude that the loss of the old bulge in *Foxc1*-cKO HFs was predicated upon enhanced proliferative activity of Bu-HFSCs, coupled with reduced E-cadherin.

Discussion

The ability to make tissues is a necessary feature of all SCs, regardless of differences in the dynamics of tissue regeneration. In vitro, many tissue SCs, including epidermal and HFSCs, can be passaged long-term without loss of their tissue-regenerating capability (19–23). In vivo, SC markers can lineage-trace progeny that survive in tissues long term (24, 25), although a recent detailed study of hematopoietic SC (HSCs) self-renewal suggests that adult homeostasis may be sustained by multiple short-term SCs that receive rare input from polyclonal long-term HSC (26, 27). In all of these cases, the outcome is long-term ability to regenerate the tissue.

Less is clear about the multiple facets that are required to balance SC use within the native tissue. Mice lacking FOXC1 in their hair coat allowed us to explore this captivating issue. In dissecting their complex phenotype that arises by the loss of a single transcription factor, we unearthed a variety of ways in which HFSCs interact with their environment to govern their proliferation and conserve their tissue-regenerating potential. Specifically, we found that FOXC1 loss in HFs causes the following: (*i*) Bu-HFSCs become primed to proliferate, as evidenced by their cell cycle status, earlier response to an activating stimuli in vivo, and increased colony forming efficiency in vitro; (*ii*) Bu-HFSCs express lower E-cadherin levels in part because of their proliferative nature; (*iii*) HFs lose their old bulge as a result of the compromised cell–cell adhesion, and fail to expand their SC numbers and thicken the animal's hair coat; (*iv*) HFs consequently accelerate their hair cycling; (*v*) When aged, HFs fail to maintain Bu-HFSC numbers and regenerate new hairs promptly, leading to a markedly sparse hair coat.

Two Is Better Than One: The Role of the Older Bulge. Our work has established an importance for the unique property of mouse pelage HFs to preserve their older bulges. Unlike WT HFs, *Foxc1*-cKO HFs always lose their prior bulge whenever they make a new one, and thus never advance past their initial starting point of having only one bulge. A critical repercussion is the loss of local inhibitory factors emanating from both $K6^+$ inner bulge (11) and suprabasal Bu-HFSCs that normally form the interface between two bulges (13). This becomes manifest in the failure of either FOXC1-deficient Bu-HFSCs or WT Bu-HFSCs in a one-bulge environment to stay in prolonged quiescence. Moreover, although ablation of *Foxc1* in a two-bulge HF did shorten the SC quiescence period, indicative of an intrinsic defect, the presence of the second bulge nevertheless delayed the precocious anagen entry of the active bulge compared with that seen in *Foxc1*-cKO one-bulge HFs. These findings are relevant in light of other HFs, such as rodent whiskers, which do not accumulate multiple bulges and, like *Foxc1*-cKO pelage HFs, also exhibit shorter telogen durations (28).

Overall, our results provide compelling evidence that prior bulges participate in regulating HFSC quiescence and hair cycling. Indeed, excessive tissue regeneration and SC expenditure have no favorable outcome in FOXC1-deficient mice, as their hair coat remains thin. Our findings suggest that furry mammals have acquired a means to generate new bulges and preserve the old ones to maintain tissue-regenerative potential for the lifetime of the animal.

It has been demonstrated that HFSCs that have undergone fewer divisions are set aside in the old bulge to participate in wound healing, whereas those with more divisions are recycled into the new bulge and tasked with homeostatic hair regeneration (11). A WT HF almost never accommodates more than four bulges. What happens to the older bulges is still unknown. An intriguing idea is that once a bulge sheds its old hair, its HFSCs with their low division history fold into the newer bulges and "rejuvenate" the HFSC pool to improve its efficiency in hair cycling and wound repair.

A Distinct Hair-Loss Mechanism. Intercellular adhesion defects are also at the root of another mouse mutant that fails to maintain its hair coat, namely mice lacking the desmosomal glycoprotein, desmoglein 3 (DSG3) (29). That said, the mechanism of bulge and club hair loss by *Foxc1*-cKO HFs seems to be distinct from *Dsg3*-KO mice, which always lose their new hair during telogen,

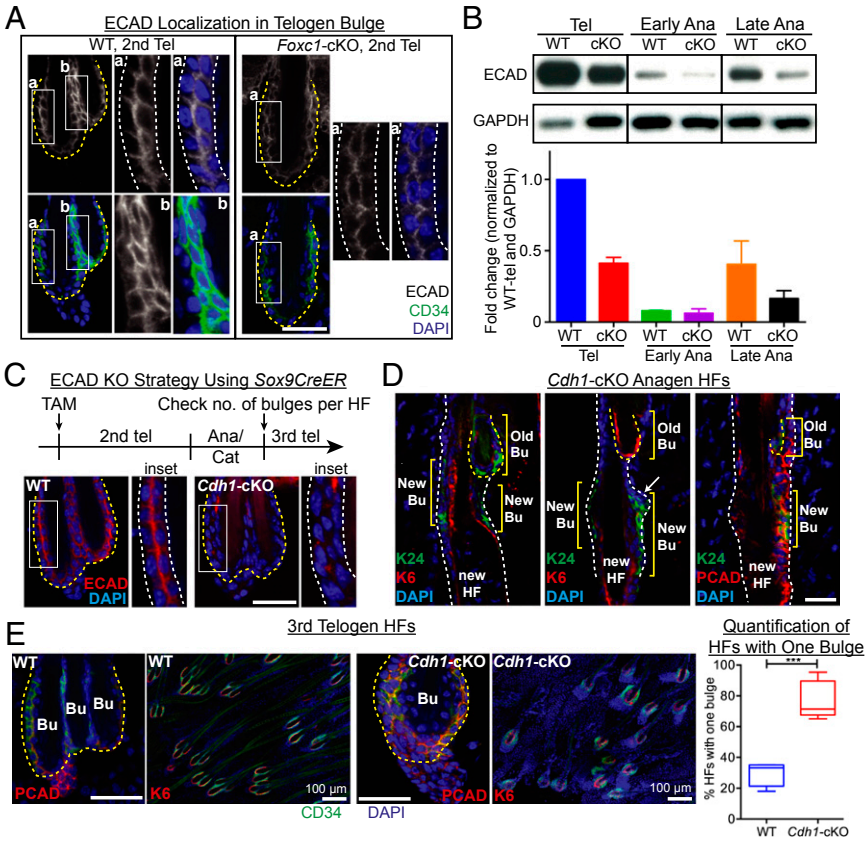

Fig. 6. Reducing intercellular junctions between HFSCs contributes to the loss of the old bulge during new hair growth. (*A*) Immunofluorescence of second telogen HFs to analyze E-cadherin localization. *Inset a* zooms in on basal-Bu-HFSC layer in both WT and *Foxc1*-cKO; note that the compacted, organized bilayer of cells, characteristic of the WT bulge, is disorganized and displays extraneous cells in the *Foxc1*-cKO bulge. *Inset b* zooms in on suprabasal-Bu-HFSC layer in WT. (Scale bar, 30 μm.) (*B*) Immunoblotting of FACS-purified Bu-HFSCs illustrates dynamic changes in E-cadherin levels during the hair cycle. Quantifications are mean ± SEM of ≥ 3 independent replicates normalized to WT-tel using GAPDH as loading control. Note that FOXC1 loss reduces overall E-cadherin levels but does not alter their dynamics during the hair cycle. (*C*) Strategy to ablate *Cdh1* gene expression in HFs by using *Sox9-CreER* mice. Immunofluorescence images depict loss of E-cadherin after tamoxifen treatment and appearance of disorganized cells within the bulge, compared with WT. (Scale bar, 30 μm.) (*D*) Immunofluorescence of sagittal sections of *Cdh1*-cKO anagen HFs depicting the position of the old bulge relative to the newly specified bulge. Arrow points to $K24^+$ cells left behind as the old bulge moved upwards. (Scale bar, 30 μm.) (*E*) Immunofluorescence of WT and *Cdh1*-cKO third telogen HFs. Quantifications show that most *Cdh1*-cKO HFs had only one bulge by their third telogen. Box-and-whisker plot: midline, median; box, 25th and 75th percentiles; whiskers, minimum and maximum ($n \geq 4$ mice, ≥80 HFs per mouse). (Scale bars, 30 μm unless indicated otherwise.) ***$P < 0.001$.

and hence undergo cyclical balding. In contrast, *Foxc1*-cKO mice lose only their old hairs (and not the newly generated hair) during anagen, and thus continuously display a new hair coat layer. Moreover, the adhesive defect in *Dsg3*-KO HFs was attributed to reduced adhesion between the two bulge layers, whereas that in *Foxc1*-cKO HFs appears to involve inter-HFSC adhesion, resulting in a failure to retain the old bulge HFSCs.

The hair loss process that occurs naturally is known as exogen, in which the club hair is shed from the HF. Because it happens infrequently in WT pelage HFs, multiple bulges accumulate. When it does happen, it largely coincides with anagen (30, 31). Interestingly, *Foxc1*-cKO HFs also lose their club hairs in late anagen. However, although exogen is thought to involve the proteolytic shedding of the club hair from the bulge in situ without loss of Bu-HFSCs (31), *Foxc1*-cKO HFs appear to lose their old bulge ($K24^+$ HFSCs, $K6^+$ inner cells, and club hair) in its entirety. Additionally, *Foxc1*-cKO bulge loss appears to take place only when subjected to a stimulus, which in the hair cycle is the mechanical force imposed by the newly growing hair during anagen. In contrast, during telogen the single bulge remains in position. As more is learned about the normal process of exogen, the extent to which *Foxc1*-cKO mice might serve as a model of premature exogen should become more apparent.

An Aged Phenotype Not Normally Observed in WT. Mouse pelage HFs use multiple strategies to keep their SCs quiescent and restrict the number of hair cycles only to what is necessary to maintain a full hair coat. As such, the hair coats of aged and young mice are usually quite similar in appearance. However, when mice are forced by repeated depilation to undergo excessive hair cycling, their hair coat greys, suggesting a deleterious impact on melanocyte SCs that are activated along with Bu-HFSCs during regeneration (32). In this regard, it is interesting that the *Foxc1*-cKO hair coat also greyed as mice aged. Because *Foxc1* ablation was restricted to the epithelium, its effects on melanocytes appeared to be a secondary consequence. Although future studies will be needed to dissect the precise mechanisms, the hair greying could reflect overuse of melanocyte SCs during the more frequent hair cycling, a failure of a smaller bulge to accommodate sufficient melanocyte SCs, or defective cross-talk between FOXC1-deficient HFSCs and WT melanocyte SCs.

In the context of HSCs, their "exhaustion" is typically determined by their decline in ability to reconstitute the entire hematopoietic system. It has been demonstrated that the less-proliferative HSCs from aged mice of longer-lived strains reconstitute the blood more efficiently than the more proliferative HSCs from aged mice of shorter-lived strains, suggesting a more rapid functional exhaustion in the latter (1). Here, we propose a

highly analogous case of HFSC exhaustion, in which FOXC1-deficient Bu-HFSCs are able to cope with tissue maintenance in young mice but, having undergone more rounds of cell division and tissue regeneration than WT, find themselves impaired in their ability to maintain their numbers and make new hairs promptly in aged mice. This is especially intriguing given that HFs naturally set aside SCs that have divided more frequently for new rounds of hair production (11), and FOXC1 loss further expends their activity.

Intercellular Adhesion, E-Cadherin, and SC Biology. The timing of bulge loss in anagen suggests that the reduction of E-cadherin leads to a weakening of intercellular connections within the bulge that are necessary to withstand the mechanical pressures of hair protrusion. In this regard, it is notable that adherens junctions are needed to organize actin-myosin–based filament networks across skin epithelial cells and are also important in sensing and activating tension-based signaling (33–35). Although the precise mechanisms involved in bulge retention remain to be elucidated and could involve more than E-cadherin, these relations provide a plausible working model for how loss of FOXC1 might be linked functionally to the reduced threshold in withstanding the mechanical tension necessary to anchor the reserve SC pool throughout subsequent hair cycles.

Our studies suggest that the proliferative nature of *Foxc1*-cKO Bu-HFSCs can partly account for their reduced E-cadherin protein levels. Thus, as evidenced in WT Bu-HFSCs, E-cadherin levels inversely correlated with cell cycle status throughout the periodic bouts of tissue regeneration. This notion is further supported by the transcriptional changes that occur in Bu-HFSCs during the hair cycle: when proliferating in early anagen, Bu-HFSCs are enriched for up-regulated genes encoding cell cycle proteins, whereas many down-regulated genes encode for cell-adhesion proteins. Conversely, when Bu-HFSCs cease proliferation in late anagen, cell cycle genes are down-regulated, whereas cell-adhesion genes are up-regulated (Dataset S3). Finally, our studies show that in late anagen, FOXC1 is necessary to re-establish Bu-HFSC quiescence and restore E-cadherin levels. In its absence, cells remain proliferative and cell-adhesion gene expression and E-cadherin levels remain low, ultimately causing the loss of the bulge and its associated consequences.

In summary, our findings best fit a model whereby the loss of FOXC1 leads to elevated cell cycle transcripts and enhanced HFSC activity. This in turn reduces E-cadherin levels, heightening the sensitivity of the old bulge to mechanical stress induced by hair growth. With each prior bulge lost during the subsequent anagen, a shortage of Bu-HFSCs and inner bulge cells arise, further accelerating HFSC activity and use by lowering the threshold for their activation. At least for the WT pelage HF in the context of its native environment, prudence in conserving stem cell activity appears to be essential to maintain its SC numbers and preserve its tissue-regenerating activity throughout the lifetime of the animal.

Materials and Methods

Mice and Procedures. *Foxc1*^{flox} mice were obtained from Tsutomu Kume (36). *K14-Cre*, *Sox9-CreER*, *Nfatc1*^{flox}, *Cdh1*^{flox} and *Rosa26*$^{Flox\text{-}Stop\text{-}Flox\text{-}YFP}$ mice were described previously (37–41). *Sox9-CreER* was activated by intraperitoneal injection of tamoxifen (75-μg/g body weight, in corn oil) once a day for 2–3 d. BrdU (Sigma; 50-μg/g body weight) was injected intraperitoneally into mice twice a day before putting mice under anesthesia to obtain a skin biopsy or before lethal administration of CO_2. For depilation experiments, molten wax was applied onto the hair coats of anesthetized mice and peeled off after hardening. For the tape assay to analyze hair adhesion, a narrow strip of cloth surgical tape of fixed length was attached onto hairs of anesthetized mice and peeled off. For the hair-dye experiment, hairs of anesthetized mice were dyed using a glow-in-the-dark red hair color cream for 30–40 min before rinsing dye off under warm water. Dyed hair coats were visualized by fluorescence under Leica dissection scope. All animals were maintained in an animal facility approved by the Association for Assessment and Accreditation of Laboratory Animal Care, and procedures were performed with protocols approved by Rockefeller University's Institutional Animal Care and Use Committee members and staff.

Hair Cycle Analysis. HFs were staged based on Müller-Röver et al. (42). To track hair cycles, full-length telogen hairs were trimmed with electric clippers to reveal back skin. HF entry into anagen was determined by darkening of skin and reappearance of hair. Completion of anagen and catagen and reentry into telogen were determined by appearance of full-length hairs and loss of pigmentation in skin. Hairs were trimmed again to observe entry into the next anagen. Mice were checked in this way twice a week for long-term monitoring of hair cycle status. Progression of first and second hair cycles in Black Swiss and C57BL/6J strains were verified to be largely similar. *Foxc1*^{flox} (Black Swiss) × *K14-Cre* (CD1) mice were back-crossed for ≥ 4 generations to pure Black Swiss mice to achieve a background strain of > 90% Black Swiss. *Foxc1*^{flox} (Black Swiss) × *Sox9CreER* × *R26-YFP* (C57BL/6J) mice were of mixed background. Hair cycle phenotypes were consistently observed in both genders of mice.

Antibodies. The following antibodies and dilutions were used: FOXC1 (guinea pig, 1:1,000; E.F. laboratory), P-cadherin (goat, 1:200; R&D Systems), CD34 (rat, 1:100; eBioscience), LHX2 (rabbit, 1:2,000; E.F. laboratory), SOX9 (rabbit, 1:1,000; E.F. laboratory), NFATC1 (mouse, 1:100; Santa Cruz), TCF4 (rabbit, 1:250; Cell Signaling), BrdU (rat, 1:100; Abcam), K6 (guinea pig, 1:2,000; E.F. laboratory), K24 (rabbit, 1:5,000; E.F. laboratory), K14 (rabbit, 1:500; E.F. laboratory), E-cadherin (rabbit, 1:5,000; Cell Signaling), GFP (chicken, 1:2000, abcam), and GAPDH (mouse, 1:2,500; Abcam). Nuclei were stained with DAPI. EdU click-iT reaction was performed according to manufacturer's directions (Thermo Fisher).

Histology and Immunofluorescence. To prepare sagittal skin sections for immunofluorescence microscopy, backskins were embedded in OCT, frozen, and cryosectioned (20 μm). Sections were fixed for 10 min in 4% (wt/vol) paraformaldehyde (PFA) in PBS at room temperature and permeabilized for 20 min in PBS + 0.3% Triton (PBST). To prepare whole-mounts for immunofluorescence microscopy, adipose tissue was scraped from backskins, which were then incubated (dermis side down) on 2.5 U/mL dispase + 20 mM EDTA for 2 h at 37 °C. Epidermis and HF were separated from dermis, fixed in 4% (wt/vol) PFA for 30 min at room temperature, and permeabilized for 30 min in 0.5% PBST. Sections and whole-mounts were blocked for 1–2 h at room temperature in 2% (vol/vol) fish gelatin, 5% (vol/vol) normal donkey serum, 1% (wt/vol) BSA, 0.2–0.3% Triton in PBS. Primary Abs were incubated overnight at 4 °C and secondary Abs conjugated to Alexa 488, 546, or 647 were incubated for 1–2 h at room temperature. Mouse antibodies were incubated with M.O.M. block according to the manufacturer's directions. Images were acquired with Zeiss Axio Observer Z1 equipped with ApoTome.2 through a 20× air objective or Zeiss LSM780 laser-scanning confocal microscope through a 40× water objective.

FACS. To prepare single-cell suspensions from telogen backskin, subcutaneous fat was scraped off with a scalpel and backskin was placed (dermis side down) on trypsin (Gibco) at 37 °C for 35–45 min. To prepare single-cell suspensions from anagen backskin, backskin was placed (dermis side down) on collagenase (Sigma) at 37 °C for 45 min, the dermal side was scraped off with a scalpel, and the remaining epidermal side was transferred to Trypsin at 37 °C for 20 min. To obtain single epithelial cell suspensions, HFs and epidermal cells were scraped off gently from all trypsinized backskins with a scalpel and filtered with strainers (70 μm, followed by 40 μm). Dissociated cells were incubated with the appropriate antibodies for 20 min at 4 °C. For cell cycle profiling, dissociated cells were fixed with 4% PFA for 30 min at room temperature and permeabilized with 0.1% PBST for 20–25 min at room temperature before antibody incubation for 20 min at room temperature. The following antibodies were used: CD34-eFluor660 (1:100; eBioscience), α6-PE (1:100; BD Biosciences), Sca1-Percp_Cy5.5 (1:1,000; eBioscience), and Ki67-Pe_Cy7 (1:400; eBioscience). DAPI was used to exclude dead cells. FxCycle violet stain (Invitrogen) was used to analyze DNA content. Cell purification was performed on FACS Aria sorters equipped with Diva software (BD Biosciences). FACS analyses were performed using LSRII FACS Analyzers and then analyzed using FlowJo program.

Cell Culture. FACS-purified HFSCs were plated in equal numbers, in triplicates, onto mitomycin C-treated dermal fibroblasts in E-media supplemented with 15% (vol/vol) serum and 0.3 mM calcium. For colony-forming efficiency assay, cells were cultured for 14 d, then fixed and stained with 1% (wt/vol) Rhodamine B (Sigma). Colony diameter and colony number were quantified using scanned images of culture plates in ImageJ. For cell-adhesion assay, FACS-purified HFSCs were plated in equal numbers, in triplicates, onto polyethylene-glycol 24-well culture plates coated with matrigel (BD Biosciences), collagen I (BD Biosciences), fibronectin (Millipore), or laminin 511 (BioLamina). After 1 h, nonadherent cells were washed off and adherent

cells were fixed with 4% PFA for 10 min at room temperature and permeabilized with 0.3% PBST. Cells were incubated with antibody against K14 overnight at 4 °C and with Odyssey secondary antibody for 1 h at room temperature. Imaging was performed on an Odyssey infrared scanner (LI-COR). Quantification of the well area occupied by $K14^+$ adherent cells was performed using ImageJ.

RNA Purification, RNA-Seq, and Quantitative RT-PCR. Total RNA was purified from FACS-purified cells by directly sorting cells in $TRIzol^{LS}$ (Sigma), followed by extraction using Direct-Zol RNA miniprep kit (Zymo Research). RNA quality was determined using an Agilent 2100 Bioanalyzer and all samples sequenced had RNA integrity numbers >8. mRNA library preparation using Illumina TrueSeq mRNA sample preparation kit and single-end sequencing on Illumina HiSEq. 2000 were performed at Weill Cornell Medical College Genomic Core Facility (New York). Alignment of reads was done using TopHat with the mm9 build of the mouse genome. Transcript assembly and differential expression were performed using Cufflinks with Refseq mRNAs to guide assembly (43). Differentially expressed genes were used in Gene Ontology (GO) term analysis to find enriched functional annotations. For real-time quantitative RT-PCR (qRT-PCR), equivalent amounts of RNA were reverse-transcribed using SuperScript III (Thermo Fisher). cDNAs were normalized to equal amounts using primers against *Ppib2*. qRT-PCR was performed with SYBR green PCR Master Mix (Sigma) on an Applied Biosystems 7900HT Fast Real-Time PCR system.

Immunoblotting. FACS-purified Bu-HFSC lysates were prepared using RIPA buffer. Gel electrophoresis was performed using 4–12% NuPAGE Bis-Tris gradient gels (Thermo Fisher) and transferred to nitrocellulose membranes (Amersham). Membranes were blocked in 5% (wt/vol) milk in PBS containing 0.1% Tween 20 for 1 h at room temperature, incubated with primary antibodies overnight at 4 °C, and with secondary antibodies conjugated with HRP for 1 h at room temperature. HRP was detected using ECL (Amersham).

Statistical Analysis. Data were analyzed and statistics were performed using unpaired two-tailed Student's *t* test and ANOVA (Prism5 GraphPad). Significant differences between the two groups are noted by asterisks (*$P <$ 0.05; **$P < 0.01$: ***$P < 0.001$; ****$P < 0.0001$).

Note Added in Proof. While our paper was in press, a similar publication appeared corroborating our finding that FOXC1 plays a key role in regulating stem cell quiescence in the hair follicle (44).

ACKNOWLEDGMENTS. We thank B. de Crombrugghe for *Sox9-CreER* mice; R. Kemler for *Cdh1* fl/fl mice; L. Glimcher for *Nfatc1* fl/fl mice; the many colleagues who donated mice to Jackson Laboratories depository; S. Mazel, S. Han, L. Li, S. Semova, and S. Tadesse for FACS (The Rockefeller University Flow Cytometry Resource Center facility, supported by the Empire State Stem Cell fund through New York State Department of Health Contract C023046); The Rockefeller University Comparative Biology Center (Association for Assessment and Accreditation of Laboratory Animal Care-accredited) for veterinary care; The Rockefeller University Bioimaging Resource Center (A. North, Director); E.F. laboratory staff members L. Polak, N. Stokes, D. Oristian, S. Jordan, M. Sribour, A. Aldeguer, and J. Levorse for their assistance in mouse research; E. Wong for her assistance in antibody generation; M. Nikolova for her assistance with cell culture; E.F. laboratory members Y.-C. Hsu and P. Chi for their discussions during the early phases of this project; and E.F. laboratory members N. Oshimori, B. Keyes, A. Asare, and E. Heller for their helpful discussions throughout this project. This work was supported by National Institutes of Health/National Institute of Arthritis and Musculoskeletal and Skin Diseases Grant R01-AR050452 (to E.F.) and partially by a grant from the Ellison Foundation. K.L. is an A-Star Predoctoral Fellow funded by the government of Singapore. E.F. is a Howard Hughes Medical Institute Investigator.

1. Orford KW, Scadden DT (2008) Deconstructing stem cell self-renewal: Genetic insights into cell-cycle regulation. *Nat Rev Genet* 9(2):115–128.
2. Cheung TH, Rando TA (2013) Molecular regulation of stem cell quiescence. *Nat Rev Mol Cell Biol* 14(6):329–340.
3. Morrison SJ, Spradling AC (2008) Stem cells and niches: Mechanisms that promote stem cell maintenance throughout life. *Cell* 132(4):598–611.
4. Hsu YC, Fuchs E (2012) A family business: Stem cell progeny join the niche to regulate homeostasis. *Nat Rev Mol Cell Biol* 13(2):103–114.
5. Chen CC, et al. (2015) Organ-level quorum sensing directs regeneration in hair stem cell populations. *Cell* 161(2):277–290.
6. Festa E, et al. (2011) Adipocyte lineage cells contribute to the skin stem cell niche to drive hair cycling. *Cell* 146(5):761–771.
7. Kfoury Y, Mercier F, Scadden DT (2014) SnapShot: The hematopoietic stem cell niche. *Cell* 158(1):228–228.e1.
8. Plikus MV, Chuong CM (2014) Macroenvironmental regulation of hair cycling and collective regenerative behavior. *Cold Spring Harb Perspect Med* 4(1):a015198.
9. Plikus MV, et al. (2008) Cyclic dermal BMP signalling regulates stem cell activation during hair regeneration. *Nature* 451(7176):340–344.
10. Keyes BE, et al. (2013) Nfatc1 orchestrates aging in hair follicle stem cells. *Proc Natl Acad Sci USA* 110(51):E4950–E4959.
11. Hsu YC, Pasolli HA, Fuchs E (2011) Dynamics between stem cells, niche, and progeny in the hair follicle. *Cell* 144(1):92–105.
12. Rhee H, Polak L, Fuchs E (2006) Lhx2 maintains stem cell character in hair follicles. *Science* 312(5782):1946–1949.
13. Blanpain C, Lowry WE, Geoghegan A, Polak L, Fuchs E (2004) Self-renewal, multipotency, and the existence of two cell populations within an epithelial stem cell niche. *Cell* 118(5):635–648.
14. Genander M, et al. (2014) BMP signaling and its pSMAD1/5 target genes differentially regulate hair follicle stem cell lineages. *Cell Stem Cell* 15(5):619–633.
15. Plikus MV, Chuong C-M (2008) Complex hair cycle domain patterns and regenerative hair waves in living rodents. *J Invest Dermatol* 128(5):1071–1080.
16. Greco V, et al. (2009) A two-step mechanism for stem cell activation during hair regeneration. *Cell Stem Cell* 4(2):155–169.
17. Horsley V, Aliprantis AO, Polak L, Glimcher LH, Fuchs E (2008) NFATc1 balances quiescence and proliferation of skin stem cells. *Cell* 132(2):299–310.
18. Tinkle CL, Lechler T, Pasolli HA, Fuchs E (2004) Conditional targeting of E-cadherin in skin: Insights into hyperproliferative and degenerative responses. *Proc Natl Acad Sci USA* 101(2):552–557.
19. Green H (1991) Cultured cells for the treatment of disease. *Sci Am* 265(5):96–102.
20. Huch M, et al. (2013) In vitro expansion of single Lgr5+ liver stem cells induced by Wnt-driven regeneration. *Nature* 494(7436):247–250.
21. Jones PH, Harper S, Watt FM (1995) Stem cell patterning and fate in human epidermis. *Cell* 80(1):83–93.
22. Sato T, Clevers H (2015) SnapShot: Growing organoids from stem cells. *Cell* 161(7):1700–1700.e1.
23. Sato T, et al. (2009) Single Lgr5 stem cells build crypt-villus structures in vitro without a mesenchymal niche. *Nature* 459(7244):262–265.
24. Barker N, et al. (2007) Identification of stem cells in small intestine and colon by marker gene Lgr5. *Nature* 449(7165):1003–1007.
25. Samokhvalov IM, Samokhvalova NI, Nishikawa S (2007) Cell tracing shows the contribution of the yolk sac to adult haematopoiesis. *Nature* 446(7139):1056–1061.
26. Busch K, et al. (2015) Fundamental properties of unperturbed haematopoiesis from stem cells in vivo. *Nature* 518(7540):542–546.
27. Sun J, et al. (2014) Clonal dynamics of native haematopoiesis. *Nature* 514(7522):322–327.
28. Ibrahim L, Wright EA (1975) The growth of rats and mice vibrissae under normal and some abnormal conditions. *J Embryol Exp Morphol* 33(4):831–844.
29. Koch PJ, et al. (1998) Desmoglein 3 anchors telogen hair in the follicle. *J Cell Sci* 111(Pt 17):2529–2537.
30. Milner Y, et al. (2002) Exogen, shedding phase of the hair growth cycle: Characterization of a mouse model. *J Invest Dermatol* 119(3):639–644.
31. Higgins CA, Westgate GE, Jahoda CA (2009) From telogen to exogen: Mechanisms underlying formation and subsequent loss of the hair club fiber. *J Invest Dermatol* 129(9):2100–2108.
32. Endou M, Aoki H, Kobayashi T, Kunisada T (2014) Prevention of hair graying by factors that promote the growth and differentiation of melanocytes. *J Dermatol* 41(8):716–723.
33. Schlegelmilch K, et al. (2011) Yap1 acts downstream of α-catenin to control epidermal proliferation. *Cell* 144(5):782–795.
34. Silvis MR, et al. (2011) α-Catenin is a tumor suppressor that controls cell accumulation by regulating the localization and activity of the transcriptional coactivator Yap1. *Sci Signal* 4(174):ra33.
35. Vasioukhin V, Bauer C, Yin M, Fuchs E (2000) Directed actin polymerization is the driving force for epithelial cell-cell adhesion. *Cell* 100(2):209–219.
36. Sasman A, et al. (2012) Generation of conditional alleles for Foxc1 and Foxc2 in mice. *Genesis* 50(10):766–774.
37. Aliprantis AO, et al. (2008) NFATc1 in mice represses osteoprotegerin during osteoclastogenesis and dissociates systemic osteopenia from inflammation in cherubism. *J Clin Invest* 118(11):3775–3789.
38. Boussadia O, Kutsch S, Hierholzer A, Delmas V, Kemler R (2002) E-cadherin is a survival factor for the lactating mouse mammary gland. *Mech Dev* 115(1-2):53–62.
39. Mao X, Fujiwara Y, Orkin SH (1999) Improved reporter strain for monitoring Cre recombinase-mediated DNA excisions in mice. *Proc Natl Acad Sci USA* 96(9):5037–5042.
40. Soeda T, et al. (2010) Sox9-expressing precursors are the cellular origin of the cruciate ligament of the knee joint and the limb tendons. *Genesis* 48(11):635–644.
41. Vasioukhin V, Degenstein L, Wise B, Fuchs E (1999) The magical touch: Genome targeting in epidermal stem cells induced by tamoxifen application to mouse skin. *Proc Natl Acad Sci USA* 96(15):8551–8556.
42. Müller-Röver S, et al. (2001) A comprehensive guide for the accurate classification of murine hair follicles in distinct hair cycle stages. *J Invest Dermatol* 117(1):3–15.
43. Trapnell C, et al. (2012) Differential gene and transcript expression analysis of RNA-seq experiments with TopHat and Cufflinks. *Nat Protoc* 7(3):562–578.
44. Wang L, Siegenthaler JA, Dowell RD, Yi R (2016) Foxc1 reinforces quiescence in self-renewing hair follicle stem cells. *Science* 351:613–617.